Nature of the parametrically excited bound soliton state

Xinlong Wang*
Institute of Acoustics, Nanjing University, Nanjing 210093, People's Republic of China
(Received 20 April 1998)

The internal dynamics of the parametrically excited bound state of double solitons is explored, in particular, the periodic ''collision'' behavior of the identical solitons. The results reveal the collapse-recreation mechanism of the endless ''collisions,'' in which momentum of each soliton always flows toward the symmetric center of the state. It is also found that damping dissipation plays an important role in maintaining the regular dynamics of ''collisions.'' In weakly dissipative media, the parametric excitation of some other internal oscillation mode of high frequency can have the soliton-soliton interaction irregular, or can even break the spatial symmetry. [S1063-651X(98)07711-3]

PACS number(s): 03.40.Kf, 47.35.+i, 47.20.Ky, 42.65.Tg

Bound states of solitons have been an active topic in soliton physics. As is well known, the bound states in the standard nonlinear Schrödinger (NLS) system are unstable due to the zero binding energy [1]. However, several recent investigations [2–7] have shown that stable bound states may exist in various perturbed NLS and related equations that are usually of the *driven-damped* type. In these systems [2–5], a combination of dispersion and dissipation effects renders the soliton tails exponentially decaying with oscillations rather than simple decaying. These tails will naturally give rise to a set of local minima of the interaction potential [1], which account for the formation of the bound states. In general, such stable bound states take the forms of the fixed points [2,3,6,7] or the infinite-period limit cycle [5] of the underlying dynamical systems. What interests us here is the *oscillatory* bound state that was experimentally observed [8,9] in Faraday's water resonator and numerically reproduced [10] with the *parametrically driven, damped nonlinear Schrödinger* (PDNLS) equation [3,11–15]

$$i(\phi_t+\alpha\phi)+\phi_{xx}+(2|\phi|^2-1)\phi+\gamma\phi^*=0, \qquad (1)$$

where α is the damping coefficient, γ the driving strength. This is a localized object of a pair of interacting (identical) solitons, and it plays the role of a ''molecule'' in the one-dimensional ordered oscillatory patterns of PDNLS multisolitons [16]. Of particular interest is the *oscillation* or the periodic ''*collision*'' behavior of the bound solitons, which most clearly demonstrates the particle character of the solitons. However, from the viewpoint of particle nature, some basic problems still remain unresolved; for example, whether the *identical* solitons exchange their places or not at the collision instants [8], or, does the soliton dynamics follow the collision model in the classic sense? On the other hand, there is a certain lack of clear understanding of the formation mechanism of this bound state. In this study we explore the internal dynamics of the bound state and its nonlinear complexity, and attempt to provide the ultimate answers to the pending questions. As before [10], we shall use the same symbolic notation for the polaronlike solitons; for instance, $S(\uparrow\uparrow)$ stands for the bound state.

As already reported [10], for a given α, $S(\uparrow\uparrow)$ is oscillatory in the parameter range $\gamma_1<\gamma<\gamma_2$; e.g., $1.0970<\gamma<1.1126$ for $\alpha=0.8$. Below the lower threshold γ_1, it collapses to a standing soliton $S(\uparrow)$, while above the upper threshold γ_2, it becomes standing. In all the cases, the solitary wave ϕ is symmetric with respect to its ''mass'' center: $\phi(x,t)=\phi(-x,t)$, where the symmetric center is assumed to be situated at $x=0$. As a result, the total momentum M vanishes [10]. In order to study the collision dynamics, here we define the momenta M_L and M_R for the left ($x<0$) and right ($x>0$) solitons, respectively, as follows:

$$M_L=-M_R, \quad M_R\equiv\frac{1}{2i}\int_0^\infty(\phi^*\phi_x-\phi\phi_x^*)dx. \qquad (2)$$

This definition is based on the experimental evidence that partitioning the fluid at $x=0$ does not change the behavior of each soliton [9]. In fact, in the context of fluid dynamics, it is straightforward to verify that M_L (M_R) is proportional to the fluid momentum in the region $x<0$ (>0) [17]. It follows from Eqs. (1) and (2) that

$$\frac{dM_{L,R}}{dt}+2\alpha M_{L,R}=\pm\left[|\phi|^4+\frac{1}{2}(|\phi|^2)_{xx}\right]\Bigg|_{x=0}. \qquad (3)$$

In addition, we also define the left (right) soliton ''position'' X_L (X_R) as the one at which Im(ϕ) or $|\phi|$ reaches maximum for $x<0$ (>0).

In the standing case ($\gamma>\gamma_2$), both X_L and X_R are time independent, and we have the steady solution to Eq. (3),

$$M_{L,R}=\pm\frac{1}{2\alpha}\left[|\phi|^4+\frac{1}{2}(|\phi|^2)_{xx}\right]\Bigg|_{x=0}. \qquad (4)$$

Since $|\phi^2|_{xx}>0$ at $x=0$ for separated solitons ($|X_L-X_R|>0$), we obtain that $M_L>0$ and $M_R<0$. It is strange that the standing $S(\uparrow\uparrow)$ can have two opposite momenta constantly flowing toward the symmetric center. As γ is increased from γ_2, the solitons are separated more and more, and thus, $M_L\downarrow 0$ and $M_R\uparrow 0$. In the oscillating case ($\gamma_1<\gamma<\gamma_2$), using

*Electronic address: xlwang@nju.edu.cn

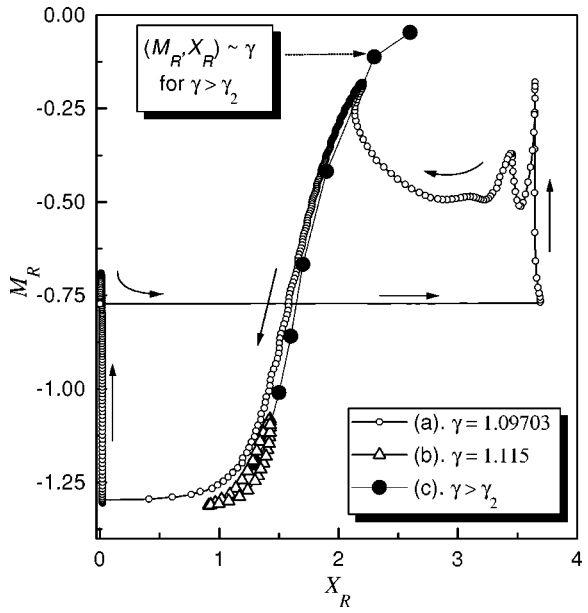

FIG. 1. (M_R, X_R) trajectories for different γ ($\alpha = 0.8$, $\ell = 40$). In the cases of (a), the identical solitons are always indistinguishable in the collision process; while in (b), they attract each other to a minimum separation, so one can always tell one from the other. With the increase of γ, the limit cycle becomes smaller and smaller, and when $\gamma > \gamma_2$, it is a γ-dependent fixed point [the line-connected solid circles (c)].

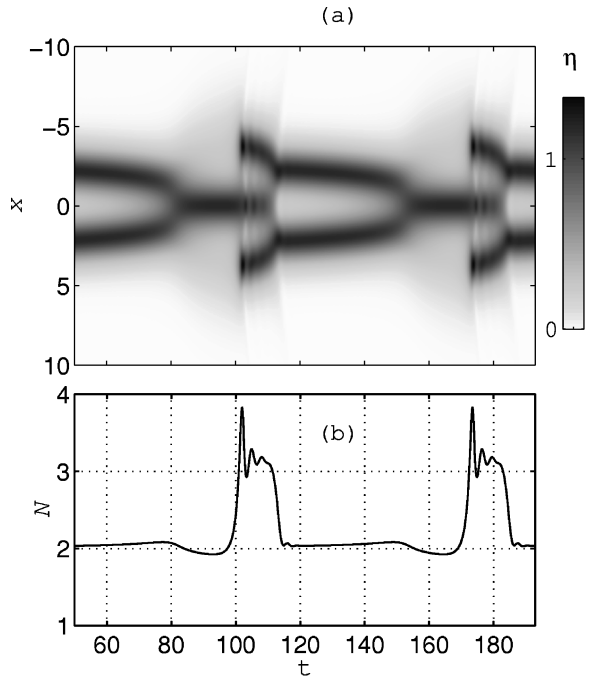

FIG. 2. Time evolution of the marginally stable $S(\uparrow\uparrow)$ [$(\alpha, \gamma) = (0.8, 1.097\,03)$, $\ell = 40$]. In (a), only the spatial portion, $-10 < x < 10$, is presented.

the numerical data obtained from the direct simulation of Eq. (1), we can easily compute the (M_L, X_L) and (M_R, X_R) trajectories. Figure 1 shows some typical cases, including the γ dependence of the fixed point (X_R, M_R) in the standing case. Unexpectedly, as we see, both M_L and M_R never reverse their directions, although the solitons seem to ''bounce back'' suddenly at each collision instant. Therefore we have $M_L > 0$ and $M_R < 0$ for any case. Undoubtedly, the result negates the usual collision model, though the collisions bear a close resemblance to the classic oscillator. It also indicates that the solitons do not penetrate through each other in the interaction.

To understand the physical significance of the intriguing phenomenon, we investigate the behavior when $S(\uparrow\uparrow)$ is of marginal stability, i.e., when γ approaches γ_1 from above. To avoid the possible influence from the boundaries (at $x = \pm \ell/2$), we select a large system size, namely, $\ell = 40$, in computer simulation. Figure 2(a) shows how the marginally stable state evolves, where $\eta = \mathrm{Im}(\phi)$, and Fig. 2(b) is the time variation of the ''particle number'' N [10]. Here N is normalized with respect to a steady soliton [16]. From the figure, one can easily identify three different stages, i.e., the *collapse* to a standing soliton ($N: 2 \to 1$), the simultaneous *recreations* of two separate solitons away from the symmetric center ($N \to 3$), and the rapid dying out of the (middle) overlapping soliton ($N: 3 \to 2$, *annihilation*). The appearances of the triple peaks (of comparable amplitudes) after collisions explain the usually overlooked phenomenon reported in the early literature [8,18]. From the figure, one can also see how $S(\uparrow\uparrow)$ is distinct from the symmetric $N = 2$ bound solitons in the integrable NLS system [19]. Undoubtedly, the energy dissipation causes the collapse (inelastic collision), while the parametric pumping contributes to the recreations (parametric amplification). Therefore the periodic ''collisions'' are actually a manifestation of the alternating internal processes, i.e., the dissipatively induced collapses and parametrically resonant recreations of the solitons. As the solitons never bounce back or pass through each other, it is certain that $M_L > 0$ and $M_R < 0$. If γ is decreased

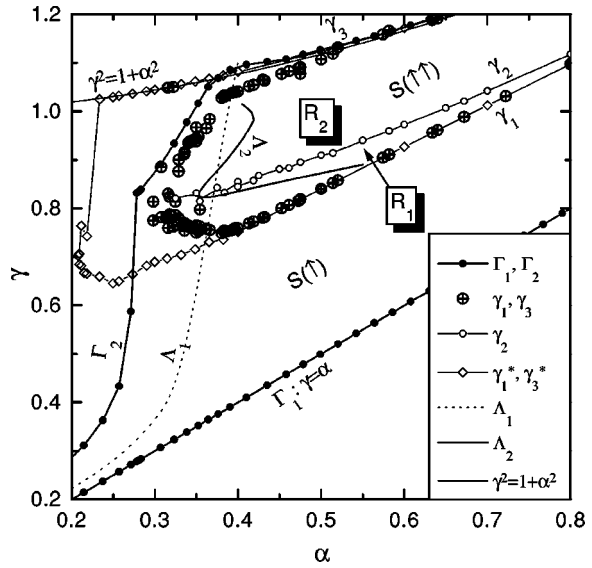

FIG. 3. Stability diagrams. The area between Γ_1 and Γ_2 is the parameter region for $S(\uparrow)$, within which Λ_1 is the Hopf bifurcation line of the state. The parameter region of $S(\uparrow\uparrow)$ is circumvented by $\otimes$'s. The curve γ_2 of the line-connected $\bigcirc$'s inside the region separates the oscillating and standing regions, R_1 and R_2, while the solid curve Λ_2 is the Hopf bifurcation line of $S(\uparrow\uparrow)$. The region bounded by the small diamonds, $\diamond$, is the extended $(R_1 + R_2)$ when the symmetry is controlled.

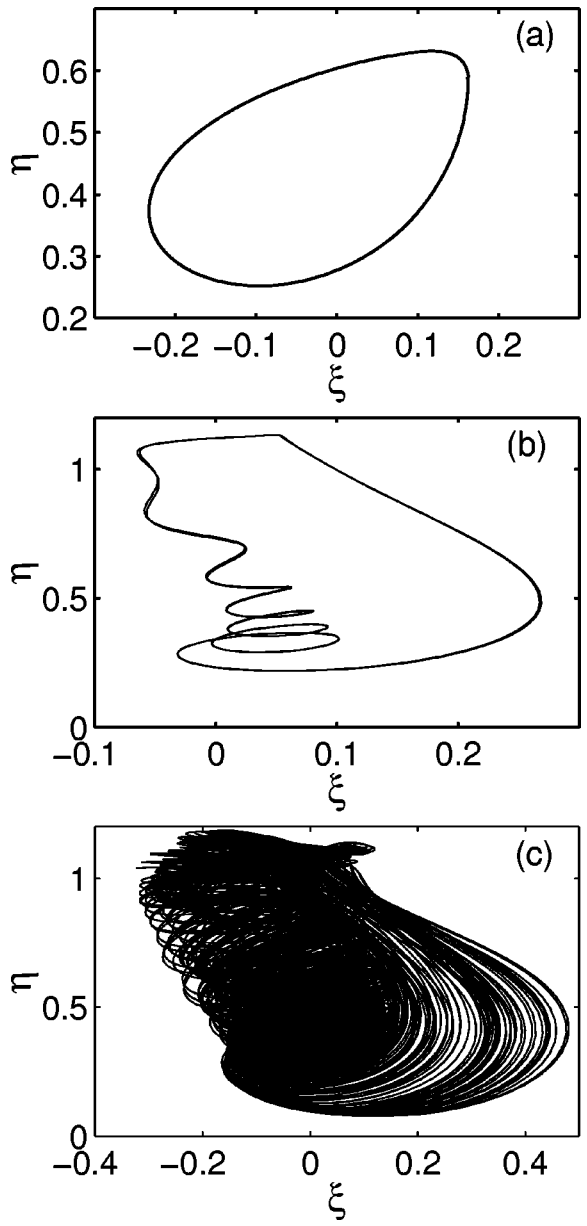

FIG. 4. Attractors of $S(\uparrow\uparrow)$, where $[\xi,\eta]=[\mathrm{Re}(\phi),\mathrm{Im}(\phi)]_{x=0}$. (a) $(\alpha,\gamma)=(0.4,0.95)\in R_2$, (b) $(\alpha,\gamma)=(0.5,0.85)\in R_2$, and (c) $(\alpha,\gamma)=(0.4,0.7669)\in R_1$ $(1000<t<1750)$.

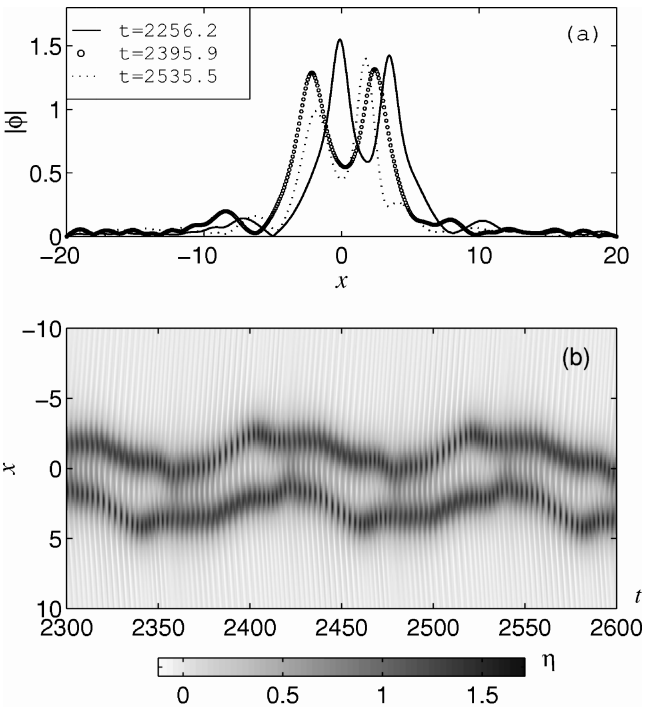

FIG. 5. (a) Broken symmetry and (b) slow swing of $S(\uparrow\uparrow)$ $[(\alpha,\gamma)=(0.35,0.8836).]$

a little, i.e., $\gamma<\gamma_1$, the input energy is not enough to regenerate the solitons, and thus $S(\uparrow\uparrow)$ transits to $S(\uparrow)$. On the other hand, if γ is increased a little, the square wave of the $N(t)$ curve becomes a series of ''spikes,'' as is the case already studied in our previous work [10]. At a stronger excitation $(\gamma>\gamma_2)$, the two reverse processes become stationary.

We find that the regular dynamics heavily depend on damping effect. Using the computed data, we have constructed the stability diagram of $S(\uparrow\uparrow)$ in the space of control parameters (α,γ), as is shown in Fig. 3 (note that this diagram is much more comprehensive than ours before [10]). Also included in the figure is the stability diagram of $S(\uparrow)$. The diagrams are calculated for the system size $\ell=40$. We have also examined several different ℓ, with various boundary conditions, but the results are almost the same for all $\ell>30$, so they are valid even for $\ell=\infty$. Our result for $S(\uparrow)$ agrees with that reported by other authors [15]. In the one-soliton state $S(\uparrow)$, an internal oscillation mode of frequency $f_h\sim 1$ is excited via a Hopf bifurcation above the dotted line Λ_1. When (α,γ) is close to the left stability boundary Γ_2, $S(\uparrow)$ exhibits some complex bifurcation behaviors leading to temporal chaos. However, it was proved [15,20] that $S(\uparrow)$ can be stably sustained in the NLS limit, $(\alpha,\gamma)\to(0,0)$, as long as (α,γ) is within the narrow parameter band just above the lower threshold Γ_1. For $S(\uparrow\uparrow)$, its whole stability region, $R_1\cup R_2$, is contained within that of $S(\uparrow)$. Because supporting $S(\uparrow\uparrow)$ requires more external energy, its lower stability boundary $\gamma=\gamma_1(\alpha)$ is high above Γ_1. Above the same upper boundary line $\gamma=\gamma_3[\approx\sqrt{(1+\alpha^2)}]$ [13,21], both $S(\uparrow)$ and $S(\uparrow\uparrow)$ are unstable with respect to continuous wave excitations. For the finite system (namely, $\ell<20$) where the boundaries significantly affect the behavior of $S(\uparrow\uparrow)$, the stability region is dependent on ℓ. Both our laboratory [9] and numerical investigations have shown that, with the decrease of ℓ, $R_1\cup R_2$ will move out of the domain for $S(\uparrow)$ in the $(+\gamma)$ direction. Since only the internal dynamics is concerned, the details of the ℓ-dependent effect will not be addressed here.

We find that the same internal oscillation of frequency f_h occurs to $S(\uparrow\uparrow)$ also, as long as (α,γ) moves across Λ_2 from the right of $R_1\cup R_2$. As compared with the collision frequency f_c, which is of order 0.1, the f_h mode is an oscillation of high frequency (hf). The bifurcation behavior depends on where (α,γ) is. Inside region R_2, the hf mode is excited as the fixed point loses its stability and is replaced by a limit cycle in relevant phase space, as shown in Fig. 4(a). In this case, $S(\uparrow\uparrow)$ becomes vibrating at frequency f_h. While in the oscillation region R_1, the hf mode appears as some trembling of the whole $S(\uparrow\uparrow)$ after each collision, which soon dies out, as shown in Fig. 4(b). In both cases,

continuous waves (cw) of small amplitude are emitted from the localized site, due to the hf vibration. Inside R_1, if (α,γ) further moves in the $(-\alpha)$ direction, then the hf mode is parametrically amplified. In this case, the strong nonlinear interaction between the f_c and f_h modes will have the collisions irregular or chaotic. As a result, the phase trajectory appears as a strange attractor, as shown in Fig. 4(c). In either R_1 or R_2, if (α,γ) comes close to the left stability boundary, $S(\uparrow\uparrow)$ can undergo a spatial bifurcation, which breaks the spatial symmetry. The broken symmetry then gives rise to the nonsymmetrical cw emission, which, in turn, causes the bound state as a whole to swing around $x=0$ slowly, as is shown in Fig. 5. When (α,γ) moves out of either R_1 or R_2 from the left stability boundary, the spatial coherent structure can no longer be preserved. Here it is quite interesting to note that we can prevent the symmetry from being broken by setting $\phi_x|_{x=0}=0$. This is equivalent to inserting a partition board at the symmetric center in experiment [9]. Consequently, the stability region of $S(\uparrow\uparrow)$ is considerably extended in the $(-\alpha)$ direction (the area bounded by γ_1^* and γ_3^* in Fig. 3). Even so, the self-destruction of $S(\uparrow\uparrow)$ is unavoidable in very weakly damping media ($\alpha<0.2$).

In conclusion, we have shown the collapse-recreation mechanism of the collision behavior of the bound solitons and the significance of damping effect in maintaining the regular dynamics. Here we give some remarks on the difference between the PDNLS bound state $S(\uparrow\uparrow)$ and those in several different but related models [2–7]. It was noted in Ref. [12] and proved in Ref. [3] that there is no oscillating tail for the PDNLS solitons due to the presence of the complex-conjugate term $\gamma\phi^*$ in Eq. (1). This has been confirmed by our experimental and numerical observations when α is sufficiently large. As a result, the interaction potential turns out to be a single-well one, rather than an oscillatory one as was usually found in the other models mentioned at the beginning. In the potential structure, if $\gamma<\gamma_1$, the attracting solitons will undergo a collapse due to energy dissipation; but when γ is a little greater than γ_1, following the collapse a pair of new solitons can be created under parametric pumping. By contrast, in the ac-driven-damped NLS system, it was observed [4] that such an oscillatory pair of solitons can only last for a finite time. Finally, we stress the special roles of damping effect in forming and maintaining $S(\uparrow\uparrow)$. Indeed, damping effect is also necessary for the formations of stable bound states in the other models mentioned at the beginning. However, for the PDNLS bound state, in addition to the direct contribution to the collision dynamics, sufficiently large damping effect can effectively suppress or attenuate the hf internal oscillation which would otherwise spoil the collision process or even destabilize $S(\uparrow\uparrow)$. This explains why in experiment $S(\uparrow\uparrow)$ is more stable and its shape looks smoother in dirty water than in clean water.

The project is supported by the NSFC under Grant No. 19774029, and the National Laboratory of Modern Acoustics in Nanjing University.

[1] V. I. Karpman and S. S. Solov'ev, Physica D **3**, 487 (1981).
[2] B. A. Malomed, Phys. Rev. A **44**, 6954 (1991).
[3] B. A. Malomed, Phys. Rev. E **47**, 2874 (1993).
[4] D. Cai, A. R. Bishop, Niels Grønbech-Jenson, and B. A. Malomed, Phys. Rev. E **49**, 1677 (1994).
[5] V. V. Afanasjev, B. A. Malomed, and P. L. Chu, Phys. Rev. E **56**, 6020 (1997).
[6] V. V. Afanasjev, Phys. Rev. E **57**, 1088 (1998).
[7] I. V. Barashenkov, Yu. S. Smirnov, and N. V. Alexeeva, Phys. Rev. E **57**, 2350 (1998).
[8] J. Wu, R. Keolian, and I. Rudnick, Phys. Rev. Lett. **52**, 1421 (1984).
[9] X. L. Wang and R. J. Wei, Phys. Lett. A **192**, 1 (1994).
[10] X. L. Wang and R. J. Wei, Phys. Rev. Lett. **78**, 2744 (1997).
[11] Y. S. Kivshar and B. A. Malomed, Rev. Mod. Phys. **61**, 763 (1989).
[12] J. W. Miles, J. Fluid Mech. **148**, 451 (1984).
[13] I. V. Barashenkov, M. M. Bogdan, and V. I. Korobov, Europhys. Lett. **15**, 113 (1991).
[14] B. Denardo, W. Wright, and S. Putterman, Phys. Rev. Lett. **61**, 1518 (1990); B. Denardo *et al.*, Phys. Rev. Lett. **68**, 1730 (1992).
[15] M. Bondila, I. V. Barashenkov, and M. M. Bogdan, Physica D **87**, 314 (1995).
[16] X. L. Wang and R. J. Wei, Phys. Rev. E **57**, 2405 (1998).
[17] In Faraday's experiment, assume that the fluid surface displacement $\xi(x,y,t)=O(\sqrt{\epsilon}\phi)$ and the velocity potential field $\Phi(x,y,z,t)=O(\sqrt{\epsilon}\phi)$ where $\phi(x,t)=O(1)$ and ϵ is a small parameter measuring the strength of nonlinearity $(0<\epsilon\ll 1)$ [12]. The fluid momentum $\vec{I}_R$ in the right region $(x>0)$ is given by $\vec{I}_R=\rho\int_0^\infty dx\int_0^b dy\int_{-d}^{\xi} dz\vec{\nabla}\Phi$ (ρ is the density of fluid, b is the breadth of the fluid channel, d is the static depth of fluid). By invoking the multiscale expansions for ξ and Φ, and averaging $\vec{I}_R$ over the fast oscillation of Faraday frequency ω, we obtain $(\omega/2\pi)\int_0^{2\pi/\omega}\vec{I}_R dt\propto\epsilon M_R\vec{e}_x+o(\epsilon)$, where $\vec{e}_x$ is the unit vector in the x direction. The same relation can also be obtained for the left soliton $(x<0)$. For the details, see, for example, X. L. Wang, Sci. China A **38**, 335 (1995).
[18] R. J. Wei *et al.*, J. Acoust. Soc. Am. **88**, 469 (1990).
[19] Hermann A. Haus and Mohammed N. Islam, IEEE J. Quantum Electron. **QE-21**, 1172 (1985).
[20] H. Friedel, E. W. Laedke, and K. H. Spatschek, J. Fluid Mech. **284**, 341 (1995).
[21] E. W. Laedke and K. H. Spatchek, J. Fluid Mech. **223**, 589 (1991).